

EVOLUTION OF ELECTRON BEAM IN THE TAPERED PLANAR WIGGLER

Soon-Kwon Nam * and Ki-Bum Kim

Department of Physics, Kangwon National University, Chunchon 200-701, Republic of Korea

Abstract

We have investigated the evolution of electron beam in the tapered planar wiggler field with a self-electric field and self-magnetic fields. In order to suppress the divergence of emittance and spread of the electron beam by the three-dimensional effects on the off-axis electron and a self-generated field effects, the tapered and bent wiggler field is applied. We calculate the emittance, transverse trajectories and Fourier transformation of electron beam using three dimensional simulation by optimizing the magnetic field strength, a tapering parameter and self-field parameters. This method could be expected to enhance the efficiency compared to those of a untapered wiggler in a free-electron laser.

INTRODUCTION

The free-electron laser which the new electromagnetic generation source have been active areas of research due to their attractive properties, such as high efficiency, tunable frequency from microwave to X-ray, and powerfull output. The quality of the electron beam plays an important role and limits the operating wavelength, gain, and efficiency.

Free-electron laser operation often requires sufficiently large gain, which increase when the beam current is increased. In the high-current regime, the electron motion can be altered by the self-generated field effects [1, 2, 3, 4, 5, 6, 7].

In this work, we study the evolution of electron beam in the tapered planar wiggler field with self-electric and self-magnetic fields. To suppress the divergence of emittance and spread of the electron beam, we apply the tapered and bent wiggler field.

The emittance, transverse trajectories and Fourier transformation of electron beam are calculated using three dimensional simulation by optimizing the magnetic field strength, a tapering parameter and self-field parameters.

THE SELF-GENERATED FIELD AND EXTERNAL MAGNETIC FIELD

The scalar potential of planar wiggler magnetic field with bent pole face is

$$\phi = -\frac{B_w}{k_w} \cosh(k_x x) \sinh(k_y y) \cos(k_w z) \quad (1)$$

and if $k_x x \ll 1$ and $k_y y \ll 1$, the wiggler magnetic field is derived from Eq. 1.

$$\mathbf{B}_w = B_w \begin{pmatrix} (1 + \frac{k_x^2 x^2}{2} + \frac{k_y^2 y^2}{2}) \cos(k_w z) \\ k_x x y \cos(k_w x) \\ -k_w y \sin(k_w x) \end{pmatrix} \quad (2)$$

In order to fulfill Maxwell's equations the scalar potential must be a solution of the Laplace equation $\nabla^2 \phi = 0$. Therefore we can find the relation such as $k_x^2 + k_y^2 = k_w^2$, and we choose the case as $k_x = k_y = k_w/\sqrt{2}$.

The vector potential of planar wiggler magnetic field which satisfy $\mathbf{B}_w = \nabla \times \mathbf{A}_w$ defined as

$$\mathbf{A}_w = -\frac{B_w}{k_w} k_x^2 x y \sin(k_w x) \hat{e}_x + \frac{B_w}{k_w} (1 + \frac{k_x^2 x^2}{2} + \frac{k_y^2 y^2}{2}) \sin(k_w z) \hat{e}_y \quad (3)$$

The space charge and current of electron beam generate the self-electric and self-magnetic fields. The Maxwell's equations in steady state are

$$\nabla \cdot \mathbf{E} = 4\pi\rho_0, \quad \nabla \times \mathbf{B} = \frac{4\pi}{c} \mathbf{J} \quad (4)$$

The self-generated electric field $\mathbf{E}_r(r)$ induced by the space charge, azimuthal self-magnetic field induced by the axial current $\mathbf{J}_z(r)$. One can find the self-generated field from the steady state Maxwell equations.

We assume that equilibrium properties (electron density and velocity) are uniform in the z-direction with $\partial n_b/\partial z = 0$ and $\partial v_b/\partial z = 0$. And there is no equilibrium electric field parallel to z-direction with $\mathbf{E} \cdot \hat{e}_z = 0$. Where n_b is electron density and v_b is mean velocity of electron. The radial density and velocity profiles are assumed to be azimuthally symmetric about the z-axis. Therefore the density and velocity profiles can be written as only function of r , which means $n_b(r, \theta, z) = n_b(r)$ and $v_b(r, \theta, z) = v_{b,z}(r) \hat{e}_z$.

There is no equilibrium electric field parallel to z-direction with $\mathbf{E} \cdot \hat{e}_z = 0$.

$$\begin{aligned} \nabla \cdot \mathbf{E}(r) &= \frac{1}{r} \frac{\partial}{\partial r} (r E_r(r)) = 4\pi\rho_0(r) \\ \nabla \times \mathbf{B}(r) &= \frac{1}{r} \frac{\partial B_\theta(r)}{\partial r} \hat{e}_z = \frac{4\pi}{c} J_z(r) \hat{e}_z \end{aligned} \quad (5)$$

where $\rho_0(r) = -ef_b(r)$ is charge density, $J_z(r) = -f_b(r)ev_z$ is axial current density, $f_b(r)$ is electron beam

* snam@kangwon.ac.kr; Tel:+82-33-250-8463; fax:+82-33-257-9689

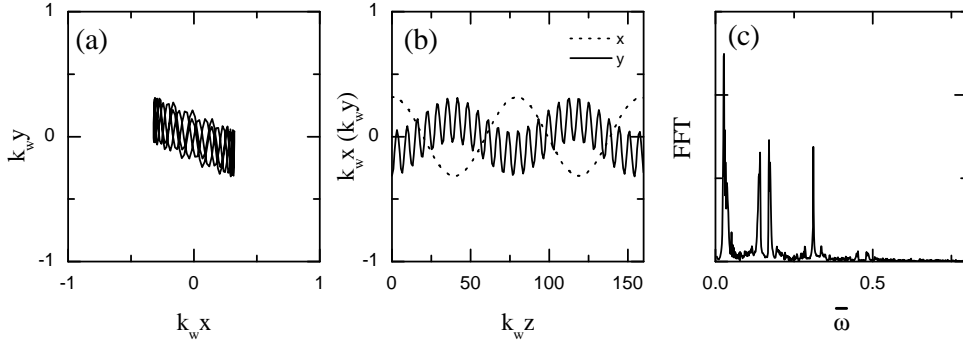


Figure 1: Electron trajectories and Fourier transformation $a_w = 1$, $\Theta = 90^\circ$ and $\kappa_s = 2$.

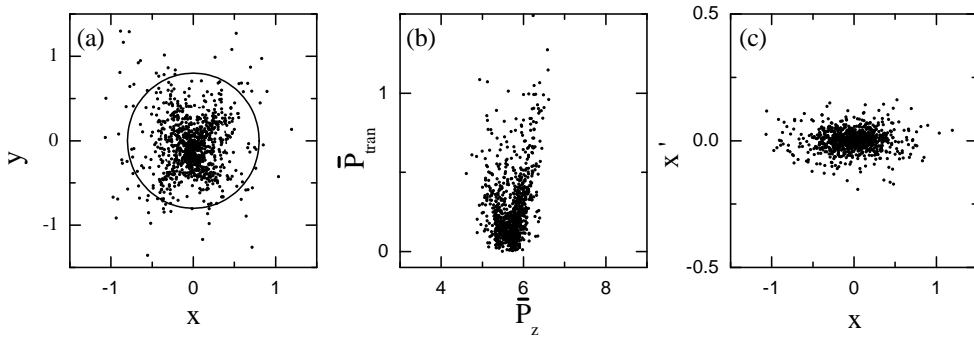


Figure 2: Electron beam profiles at the exit of the wiggler with (a) electron beam cross section, (b) transverse momentum variation and (c) x versus x' phase space. Other electron beam parameter are $a_w = 1$, $\Theta = 90^\circ$ and $\kappa_s = 2$. Dotted(solid) line indicate $r = r_b(2r_b)$.

profile function and $\beta_b = v_b/c$ is the normalized axial velocity of electron.

The self-generated field amplitude depend on the electron beam profile. We consider Gaussian shape electron beam. The profile function $f_b(r)$ for the Gaussian density is

$$f_b(r) = \frac{c_n n_b}{\sqrt{2\pi r_b^2}} \exp\left(-\frac{r^2}{2r_b^2}\right) \quad (6)$$

where n_b is electron density, $c_n = \pi r_b^2$ is the normalized factor and the self electric and magnetic field are

$$\begin{aligned} \mathbf{E}_r^s(\mathbf{r}) &= -\frac{2\alpha r_b^2}{r} \left[1 - \exp\left(-\frac{r^2}{2r_b^2}\right)\right] \hat{e}_r \\ \mathbf{B}_\theta^s(\mathbf{r}) &= -\frac{2\alpha\beta_b r_b^2}{r} \left[1 - \exp\left(-\frac{r^2}{2r_b^2}\right)\right] \hat{e}_\theta \end{aligned} \quad (7)$$

where $\alpha = \pi e n_b$, $\omega_p = (4\pi n_b e^2 / m_e)^{1/2}$ is plasma frequency of electron beam, $\omega_r = k_w c \beta$ is the angular veloc-

ity, r_b is the electron beam radius and r_w is the cylindrical waveguide radius.

The scalar potential and vector potential of the self-generated field which satisfies $\mathbf{E}_s = -\nabla\Phi_s$ and $\mathbf{B}^s = \nabla \times \mathbf{A}^s$ are

$$\begin{aligned} \Phi_s &= \alpha r_b^2 \left[\Gamma - \text{Ei}\left(-\frac{r^2}{2r_b^2}\right) - \log\left(\frac{r^2}{2r_b^2}\right) \right] \\ \mathbf{A}_\theta^s &= \Phi_s \beta_b \hat{e}_z \end{aligned} \quad (8)$$

where $\text{Ei}(x) = \int_{-\infty}^x \frac{e^{-u}}{u} du$ is exponential integrate function, and $\Gamma = \lim_{m \rightarrow \infty} (\sum_{k=1}^m \frac{1}{k} - \log m) \approx 0.577$ is Euler-Mascheroni constant.

HAMILTONIAN FORMALISM

The Hamiltonian of relativistic test electron is

$$\mathbf{H} = \sqrt{(c\mathbf{P} + e\mathbf{A})^2 + m_e^2 c^4} - e\Phi_s \equiv \gamma m_e c^2 - e\Phi_s \quad (9)$$

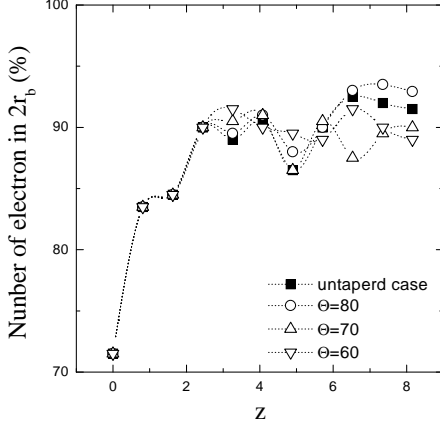


Figure 3: Number of electron along the z-axis of wiggler in $2r_b$ for various tapering parameter Θ of wiggler field. Other parameters are $a_w = 1$ and $\kappa_s = 2$.

where \mathbf{P} is the canonical momentum, $\mathbf{p} = \mathbf{P} + e\mathbf{A}/c$ is the mechanical momentum, $\gamma = \sqrt{1 + (\mathbf{p}/m_e c)^2}$ is the relativistic mass factor, m_e is the electron rest mass, e is the electron charge and total vector potential is $\mathbf{A} = \mathbf{A}_w + \mathbf{A}_\theta^s + \mathbf{A}_z^s$.

Conveniently, we introduce the dimensionless potentials, canonical momentum, and Hamiltonian defined by

$$\bar{\mathbf{A}} = \frac{e\mathbf{A}}{m_e c^2 k_w}, \quad \bar{\Phi}_s = \frac{e\Phi_s}{m_e c^2 k_w}, \quad \bar{\mathbf{P}} = \frac{\mathbf{P}}{m_e c}, \quad \bar{\mathbf{H}} = \frac{\mathbf{H}}{m_e c^2} \quad (10)$$

In the dimensionless scalar and vector potential of self-field, the constant α becomes $\alpha = \kappa_s k_w^2 / 4$, where $\kappa_s = \omega_p^2 / c^2 k_w^2$ is the dimensionless strength of the self-field. Therefore the dimensionless Hamiltonian is

$$\begin{aligned} \bar{\mathbf{H}} &= \sqrt{1 + (\bar{\mathbf{P}} + \bar{\mathbf{A}})^2} - \bar{\Phi}_s = \sqrt{1 + \Sigma h_i^2} - \bar{\Phi}_s \\ h_1 &= \bar{P}_x + k_x^2 x y \sin(k_w x) \\ h_2 &= \bar{P}_y + \left(1 + \frac{k_x^2 x^2}{2} + \frac{k_y^2 y^2}{2}\right) \sin(k_w z) \\ h_3 &= \bar{P}_z + \bar{A}_z^s \end{aligned} \quad (11)$$

where $a_w = eB_w / m_e c^2 k_w$ is a dimensionless wiggler field amplitude. To correct the electron energy loss in wiggler, the wiggler magnetic field is tapered as $a_w(z) = a_w(0)f_t(z)$, where $f_t(z)$ is the tapering profile function

$$f_t(z) = \begin{cases} 1 & \text{for } 0 \leq z < z_t \\ 1 + c_n(z - z_t) \cos \Theta & \\ + (z - z_t)^2 \cos^2 \Theta & \text{for } z > z_t \end{cases} \quad (12)$$

where z_t is the starting position of wiggler tapering, Θ is taper parameter, and c_n is constant which satisfy $f_t(z = z_f, \Theta = 45^\circ) = 1/2$.

The electron orbits can be calculated from the equations of motion which are derived from the Hamiltonian of Eq. 11. Fig. 1 shows the electron trajectories in (a) the $(k_w x, k_w y)$ plane and (b) $(k_w x(k_w y), k_w z)$ plane, and (c) the Fourier transformation for a single electron and untapered wiggler case. Other parameters are $a_w = 1$ and $\kappa_s = 2$ which correspond to the wiggler magnetic field strength $B_w = 1.78$ kG and the electron beam current $I_b = 1.47$ kA for wiggler period $\lambda_w = 6$ cm and electron beam radius $r_b = 0.4$ cm. In the planar wiggler with bent pole face, the electrons move periodically not only y direction but x direction.

We made the incident electron beam using the beam parameters such as electron beam energy $E_b = 3$ MeV, energy spread $E_s = 5\%$, emittance $\epsilon_{x,y} = 10 \pi \text{ mm} \cdot \text{mrad}$.

Fig. 2 shows the electron beam cross section, transverses momentum variation and x versus x' phase space at the exit of the wiggler with $a_w = 1$, $\Theta = 90^\circ$ and $\kappa_s = 2$.

The number of electron along z-axis of the wiggler in $2r_b$ for the various wiggler parameter Θ is shown in Fig. 3. The number of electron for the case of the tapered wiggler is increased about 1.6% compared to that of untapered case. The wiggler tapering parameter of $\Theta = 80^\circ$ was used.

STEADY-STATE SOLUTION

Assume that y component of canonical momentum $\bar{P}_y = p_y - eA_y/c$ is exact constant of the motion. Therefore, we assume that $\bar{P}_y = 0$ (i.e. $p_y = eA_y/c$) and interest the (x, z) plane only. The Hamiltonian of Eq. 11 become

$$\begin{aligned} \bar{\mathbf{H}} &= \left(1 + \bar{P}_x^2 + \left((1 + k_x^2/2) \sin(k_w z)\right)^2 \right. \\ &\quad \left. + (\bar{P}_z + \bar{A}_z^s)^2\right)^{1/2} - \bar{\Phi}_s \end{aligned} \quad (13)$$

We can find the steady-state solution $\bar{P}_z = 0, k_w z = \pi/2$ which satisfy $\bar{r}' = \psi' = \bar{P}_r' = \bar{P}_\psi' = 0$ from the equations of motion derived from the Hamiltonian.

$$\gamma = \left(1 + \left(1 + \frac{k_x^2 x^2}{2}\right)^2 + (\bar{P}_z + \bar{A}_z^s)^2\right)^{1/2} \quad (14)$$

One can find the $k_w x_0$ from Eq. 14.

Fig. 4 shows Poincaré surface of section plot in $(k_w z, \bar{P}_z)$ plane at $\bar{p}_x = 0$ for various tapering parameters and $k_w x_0$. In the strong wiggler field regime, the electron orbits for tapered wiggler $\Theta = 80^\circ$ are more stable than those of a untapered wiggler case.

CONCLUSION

We investigated the evolution of electron beam in the tapered planar wiggler field with a self-electric field and self-magnetic fields. To suppress the divergence of emittance and spread of the electron beam by the three-dimensional effects on the off-axis electron and a self-generated field effects, the tapered and bent wiggler field was applied. We calculated the emittance, transverse trajectories, Fourier

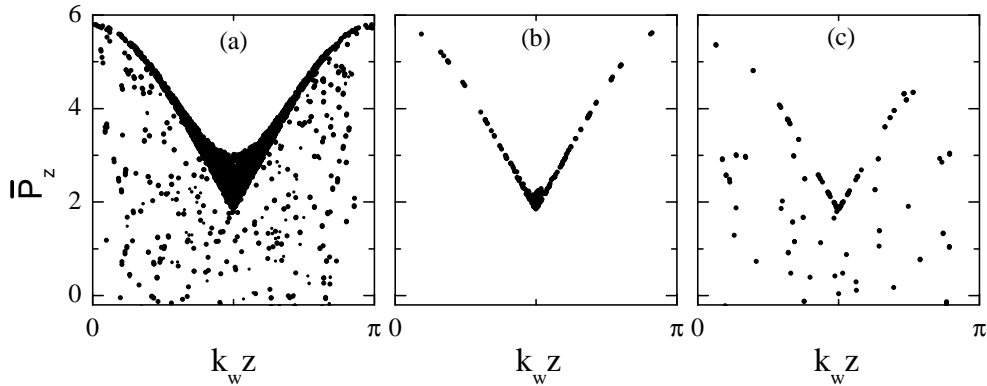


Figure 4: Poincaré surface of section plot in the $(k_w z, \bar{P}_z)$ plane at $\bar{p}_x = 0$ for (a) $\Theta = 80^\circ$ and the various $k_w x_0$, (b) $\Theta = 80^\circ$ and $k_w x_0 = 0.615$ and (c) $\Theta = 90^\circ$ and $k_w x_0 = 0.615$. Other parameters are $a_w = 5$, $k_w r_b = 0.4$ and $E_b = 3$ MeV.

transformation and Poincaré surface of section of electron beam using three dimensional simulation by optimizing the magnetic field strength and a tapering parameter of axial guide field. This method could be expected to enhance the efficiency compared to those of a untapered wiggler in a free-electron laser.

ACKNOWLEDGEMENTS

This work was supported by a Korea Research Foundation grant.

REFERENCES

- [1] C. Chen and R. C. Davidson, Phys. Fluids. **B2** (1990) 171.
- [2] C. Chen and R. C. Davidson, Phys. Rev. **A43** (1991) 5541.
- [3] L. Michel, A. Bourdier and J. M. Buzzi, Nucl. Instr. and Meth. **A304** (1991) 465.
- [4] S. Spindler and G. Renz, Nucl. Instr. and Meth. **A304** (1991) 492.
- [5] L. Michel-Lours, A. Bourdier and J. M. Buzzi, Phys. Fluids. **B5** (1993) 965.
- [6] A. Bourdier and L. Michel-Lours, Phys. Rev. **E49** (1994) 49.
- [7] R. C. Davidson, *Physics of Nonneutral Plasmas* (Addison Wesley, 1990).